An Investigation on Narrow Band PLC-Wireless Parallel Channel Capacity

Victor Fernandes[1], Mateus L. Filomeno[1], Weiler A. Finamore[1] and Moisés V. Ribeiro[1,2]

***Abstract*— This work aims to investigate achievable data rate of a hybrid narrow band (NB) communication system composed of *Power Line Communications* (PLC) and wireless channels. With this regards, we present the equations of channel capacity when using only a linear and time invariant (LTI) PLC, linear and time varying (LTV) PLC or wireless channels. Therefore, the parallel use of PLC-wireless channels capacity is deduced. Results of PLC-wireless achievable data rate are shown when both PLC and wireless channels use optimal power allocation. Furthermore, we show that the parallel use of PLC and wireless channels always present a better achievable data rate than the sole use of PLC or wireless channels.**

***Keywords*— Channel capacity, power line communications, wireless.**

I. INTRODUCTION

Electric power grids are not only useful for energy delivery but also for data communication. Recent advances in telecommunications field made possible the development of new generation of power line communication (PLC) technology for smart grid (SG) and internet of things (IoT). On the other hand, wireless communication systems are also included in this context due to several and well-established justifications which are supporting their worldwide dissemination. Both technologies (PLC and wireless) make use of the existing media to transmit data, making it easiest and costless to implement.

The signal propagation through the electric power grids suffers the effects of multipath, fading, frequency and time selectivities. This occurs when the transmitted signal traveling from one point to another in power cable faces impedance mismatch along its path and it comes from the broadcast signal propagation characteristic of electric power grids. Also, construction of power cables and dynamic of loads connected to electric power grids severely interfere with the signal propagation. On the other hand, wireless channels suffers from 3 different propagation effects: *reflection*, *scattering* and *diffraction*. The first one occurs when the propagation wave meets a very large object in comparison to its wavelength. On the contrary, *scattering* happens when the the propagation wave meets a very small object in comparison to its wavelength. *Diffraction* occurs when the signal passes through a sharpened object and it is responsible of having non-line-of-sight (NLOS) communications. Also, the random nature of wireless channels impose more difficult for data communication.

[1]Department of Electrical Engineering, Federal University of Juiz de Fora, Juiz de Fora-MG, Brazil. [2]Smarti9 Ltda., Juiz de Fora-MG. E-mails: victor.fernandes@engenharia.ufjf.br, mateus.lima@engenharia.ufjf.br, finamore@ieee.org, mribeiro@engenharia.ufjf.br. This work was partially supported by CAPES.

The sole use of PLC or wireless technology to fulfill the needs and demands related to SG and IoT is widely known. However, the lack of reliability over such channels, has push forward the investigation of the existing diversity between PLC and wireless channels to improve telecommunication system performance. In this way, the so-called PLC-wireless channel is being investigated. In [1], was shown that the PLC technology can enhance the capacity of wireless networks even using very low transmission power. Furthermore, [2] pointed out that PLC system is a promising candidate to enhance wireless relaying schemes that are based on inter-relay-communication. Also, [3] considered an ideal multi-channel receiver which is able to communicate through both wireless and PLC channels. On the other hand, [4] used link throughput analysis to show that PLC-wireless diversity can be used to minimize the likelihood of low throughput links. Moreover, [5] showed that coding diversity has the potential to offer very high throughput communications using PLC and wireless links. Finally, [6] considered the parallel use of PLC and wireless communication networks with multihop relaying and showed that the proposed schemes provide enhanced performance compared to the separate use of relays in the PLC and wireless channels.

Aiming to deepen the understanding of the usefulness of PLC-wireless channel for SG and IoT applications, this work focuses on the achievable data rate analysis of the industrial, scientific, and medical (ISM) frequency band together with the narrowband PLC frequency band. We carry out numerical simulation when the PLC channel is time invariant and time-varying perturbed by Gaussian random noise. The reported result shows that for these frequency bands, the existing diversity between both ISM and narrowband PLC channels may benefits SG and IoT applications.

II. SYSTEM MODEL

Our scenario is shown in Fig. 1. The source (S) node is communicating with the destination (D) node over two distinct channels: PLC and wireless. It is important to point out that both channels operate with a 500 kHz bandwidth, the narrowband PLC communication operates in the baseband and NB-Wireless communication operates at 915 MHz center frequency.

Fig. 1. Source-Destination link using PLC and wireless channels.

We assume that the output of the discrete-time, linear and time invariant (LTI) PLC channel, linear and time varying (LTV) PLC channel and, LTV wireless channel are given by, respectively

$$y^{P,LTI}[n] = \sum_{m=0}^{L_P-1} \sqrt{E^P} h^P[m]x[n-m] + v^P[n], \quad (1)$$

$$y^{P,LTV}[n] = \sum_{m=0}^{L_P-1} \sqrt{E^P} h^P[m,n]x[n-m] + v^P[n], \quad (2)$$

$$y^{W}[n] = \sum_{m=0}^{L_W-1} \sqrt{E^W} h^W[m,n]x[n-m] + v^W[n], \quad (3)$$

where $\{h^q[n]\}_{i=0}^{m}$ and $\{v^q[n]\}$, refer to the channel impulse response (CIR) and the additive noise and, $q \in \{P, W\}$ denotes PLC and wireless, respectively. Also, $\{x[n]\}$, L_q and E^q denote the transmission signal, the length of the CIR and the transmission energy given to the signal that will travel through the q channel, respectively. In the following, we assume that the both PLC and wireless channel are invariant during on symbol period.

Given the discrete-time vectorial representation of the CIR of the channels, $\mathbf{h}^q = [h_0^q, h_1^q, \ldots, h_{L_q-1}^q]^T$, let us denote $\mathbf{H}^q = [H^q[0], H^q[1], \ldots, H^q[N-1]]^T$, which is the discrete Fourier transform (DFT) of the CIR of the channel with length N, i.e., $\mathbf{H}^q = \boldsymbol{\mathcal{F}}[\mathbf{h}^q, \mathbf{0}_{N-L_q}]^T$, in which $\boldsymbol{\mathcal{F}}$ is the DFT matrix. We also define the diagonal matrices $\boldsymbol{\mathcal{H}}^q = \mathbf{diag}\{H^q[0], H^q[1], \ldots, H^q[N-1]\}$ and $\boldsymbol{\Lambda}_{|\boldsymbol{\mathcal{H}}^q|^2} = \mathbf{diag}\left\{|H^q[0]|^2, |H^q[1]|^2, \ldots, |H^q[N-1]|^2\right\}$ for further using. Moreover, the joint probability $p(|H^q[0]|^2, |H^q[1]|^2, \ldots, |H^q[N-1]|^2) = p(|H^q[0]|^2)p(|H^q[1]|^2)\ldots p(|H^q[N-1]|^2)$, because we assume that $H^q[i]$ and $H^q[j]$, $\forall i \neq j$ are independent random variables.

The representation of a symbol, after digital modulation, is given by $\mathbf{X} \in \mathbb{C}^{N\times 1}$, and $\mathbf{V}^q \in \mathbb{C}^{N\times 1}$, the additive noise frequency domain representation. Besides, we have $\boldsymbol{\Lambda}_{P^q} = \mathbf{diag}\left\{p_0^q, p_1^q, \ldots, p_{N-1}^q\right\}$, as a matrix representation of power allocation, so that $\mathrm{Tr}(\boldsymbol{\Lambda}_{P^q}) = P^q$, where $\mathrm{Tr}(\cdot)$ denotes the trace operation and, P^q the power allocated to the q signal. Therefore, $\boldsymbol{\Lambda}_{\sqrt{P^q}} = \mathbf{diag}\left\{\sqrt{p_0^q}, \sqrt{p_1^q}, \ldots, \sqrt{p_{N-1}^q}\right\}$ denotes the amplitude the transmitted symbol through the q channel. Note that $P = P^P + P^W$ is the total transmission power.

We considerer that $\mathbb{E}\{\mathbf{X}\} = 0$, $\mathbb{E}\{\mathbf{X}\mathbf{X}^\dagger\} = \boldsymbol{\Lambda}_{\sigma_X^2} = \mathbf{I}_N$, in which $\mathbf{I}_N$ denotes the $N \times N$ identity matrix, $\mathbb{E}\{\cdot\}$ is the expectation operator and $\dagger$ is the conjugate transpose operator. Also, $\mathbb{E}\{\mathbf{V}\} = 0$ and $\mathbb{E}\{\mathbf{V}\mathbf{V}^\dagger\} = \boldsymbol{\Lambda}_{\sigma_{\mathbf{V}}^2} = \mathbf{diag}\left\{\sigma_V^2[0], \sigma_V^2[1], \ldots, \sigma_V^2[N-1]\right\}$. Moreover, similar to [9], we assume that N-block circular Gaussian relay channel (N-CGRC). As $N \longrightarrow \infty$, the achievable data rate of the N-CGRC can be made arbitrarily close to that of the linear Gaussian relay channel (LGRC) [9].

III. Achievable data rate: PLC channel

This section introduces closed-form expressions for the achievable data rate of the LTI PLC channel and ergodic channel capacity of the LTV PLC channel.

A. LTI PLC Channel

The output of the PLC channel is given by

$$\begin{aligned} \mathbf{Y}^P &= \boldsymbol{\Lambda}_{\sqrt{P^P}} \boldsymbol{\mathcal{H}}^P \mathbf{X} + \mathbf{V}^P \\ &= \mathbf{A}^P \mathbf{X} + \mathbf{B}^P \mathbf{V}^P, \end{aligned} \quad (4)$$

where $\mathbf{A}^P = \boldsymbol{\Lambda}_{\sqrt{P^P}} \boldsymbol{\mathcal{H}}^P$ and, $\mathbf{B}^P = \mathbf{I}_N$.

Let $h(p)$ denotes the entropy of random variable p, the mutual information between the transmitted and received signals is

$$\begin{aligned} I(\mathbf{X}, \mathbf{Y}) &= h(\mathbf{Y}) - h(\mathbf{Y}|\mathbf{X}) \\ &= h(\mathbf{Y}) - (h(\mathbf{A}\mathbf{X}|\mathbf{X}) + h(\mathbf{B}\mathbf{V}|\mathbf{X})) \\ &= h(\mathbf{Y}) - h(\mathbf{B}\mathbf{V}). \end{aligned} \quad (5)$$

At this point, for simplicity, the notation $\mathbf{V}$ represents the PLC additive noise, before called $\mathbf{V}^P$. Due to the mentioned considerations, the received signal $\mathbf{Y}$ is a complex Gaussian vector. Therefore, according to [9] the entropy of $\mathbf{Y}$ is given by

$$h(\mathbf{Y}) = \log_2[(\pi e)^N \det(\mathbf{R}_{\mathbf{YY}})], \quad (6)$$

where

$$\begin{aligned} \mathbf{R}_{\mathbf{YY}} &= \mathbb{E}\{\mathbf{Y}\mathbf{Y}^\dagger\} \\ &= \mathbf{A}^P \mathbf{R}_{\mathbf{XX}} \mathbf{A}^{P\dagger} + \mathbf{B}^P \mathbf{R}_{\mathbf{VV}} \mathbf{B}^{P\dagger}. \end{aligned} \quad (7)$$

Due to the Gaussianity of the additive noise,

$$h(\mathbf{B}\mathbf{V}) = \log_2[(\pi e)^N \det(\mathbf{B}^{\mathbf{P}} \mathbf{R}_{\mathbf{VV}} \mathbf{B}^{\mathbf{P}\dagger})],$$

thus, from (5), we have

$$I(\mathbf{X}, \mathbf{Y}) = \log_2 \left[\det(\mathbf{I}_N + \mathbf{A}^P \mathbf{R}_{\mathbf{XX}} \mathbf{A}^{P\dagger} (\mathbf{B}^{\mathbf{P}} \mathbf{R}_{\mathbf{VV}} \mathbf{B}^{\mathbf{P}\dagger})^{-1})\right]. \quad (8)$$

Finally, the achievable data rate is given by

$$C^{P,LTI} = \max_{\boldsymbol{\Lambda}_{P^P}} \frac{B}{N} \log_2 [\det(\mathbf{I}_N + \mathbf{C}^P \mathbf{D}^{P^{-1}})], \quad (9)$$

subject to $\mathrm{Tr}(\boldsymbol{\Lambda}_{P^P}) \leq P$, where

$$\begin{aligned} \mathbf{C}^P &= \mathbf{A}^P \mathbf{R}_{\mathbf{XX}} \mathbf{A}^{P\dagger} \\ &= \boldsymbol{\Lambda}_{P^P} \boldsymbol{\Lambda}_{|\boldsymbol{\mathcal{H}}^P|^2} \boldsymbol{\Lambda}_{\sigma_{\mathbf{X}}^2} \end{aligned} \quad (10)$$

and

$$\begin{aligned} \mathbf{D}^P &= \mathbf{B}^P \mathbf{R}_{\mathbf{V}^P\mathbf{V}^P} \mathbf{B}^{P\dagger} \\ &= \boldsymbol{\Lambda}_{\sigma_{\mathbf{V}^P}^2}. \end{aligned} \quad (11)$$

B. LTV PLC Ergodic Channel Capacity

If we assume that PLC is LTI during one symbol period, the ergodic channel capacity of a fading LTV PLC channel is given by

$$\begin{aligned} C^{P,LTV} &= \max_{\boldsymbol{\Lambda}_{P^P}} \frac{B}{N} \mathbb{E}\{\log_2 [\det(\mathbf{I}_N + \mathbf{C}^P \mathbf{D}^{P^{-1}})]\} \\ &= \max_{\boldsymbol{\Lambda}_{P^P}} \int_0^\infty \cdots \int_0^\infty \log_2 [\det(\mathbf{I}_N + \mathbf{C}^P \mathbf{D}^{P^{-1}})] \times \\ &\quad p(|H^P[0]|^2, |H^P[1]|^2, \ldots, |H^P[N-1]|^2) \\ &\quad d|H^P[0]|^2, d|H^P[1]|^2, \ldots, d|H^P[N-1]|^2 \end{aligned} \quad (12)$$

subject to $\mathrm{Tr}(\boldsymbol{\Lambda}_{P^P}) \leq P$, in which $\mathbf{C}^P$ and $\mathbf{D}^P$ are given by (10) and (11), respectively.

IV. ACHIEVABLE DATA RATE: WIRELESS CHANNEL

This section presents closed-form expression for ergodic capacity of the LTV wireless channel.

Similarly to the PLC channel, the output of the wireless channel is given by

$$\begin{aligned}\mathbf{Y}^W &= \mathbf{\Lambda}_{\sqrt{P^W}}\boldsymbol{\mathcal{H}}^W\mathbf{X} + \mathbf{V}^W \\ &= \mathbf{A}^W\mathbf{X} + \mathbf{B}^W\mathbf{V}^W,\end{aligned} \tag{13}$$

where $\mathbf{A}^W = \mathbf{\Lambda}_{\sqrt{P^W}}\boldsymbol{\mathcal{H}}^W$ and $\mathbf{B}^W = \mathbf{I}_N$.

Then, the ergodic channel capacity of a fading LTV wireless channel is given by

$$\begin{aligned}C^W &= \max_{\mathbf{\Lambda}_{P^W}} \frac{B}{N}\mathbb{E}\{\log_2[\det(\mathbf{I}_N + \mathbf{C}^W\mathbf{D}^{W^{-1}})]\} \\ &= \max_{\mathbf{\Lambda}_{P^W}} \int_0^\infty \cdots \int_0^\infty \log_2[\det(\mathbf{I}_N + \mathbf{C}^W\mathbf{D}^{W^{-1}})] \times \\ &\quad p(|H^W[0]|^2, |H^W[1]|^2, \ldots, |H^W[N-1]|^2) \\ &\quad d|H^W[0]|^2, d|H^W[1]|^2, \ldots, d|H^W[N-1]|^2\end{aligned} \tag{14}$$

subject to $\mathrm{Tr}(\mathbf{\Lambda}_{P^W}) \leq P$, where

$$\begin{aligned}\mathbf{C}^W &= \mathbf{A}^W\mathbf{R}_{\mathbf{XX}}\mathbf{A}^{W^\dagger} \\ &= \mathbf{\Lambda}_{P^W}\mathbf{\Lambda}_{|\boldsymbol{\mathcal{H}}^W|^2}\mathbf{\Lambda}_{\sigma^2_{\mathbf{X}}}\end{aligned} \tag{15}$$

and

$$\begin{aligned}\mathbf{D}^W &= \mathbf{B}^W\mathbf{R}_{\mathbf{V}^W\mathbf{V}^W}\mathbf{B}^{W^\dagger} \\ &= \mathbf{\Lambda}_{\sigma^2_{\mathbf{V}^W}}.\end{aligned} \tag{16}$$

V. PLC-WIRELESS CHANNEL CAPACITY

This section presents closed-form expressions for ergodic capacity of the LTI PLC-wireless and LTV PLC-wireless channels.

The received symbol of the hybrid receiver, can be expressed as

$$\begin{aligned}\mathbf{Y} &= \begin{bmatrix}\mathbf{Y}^P \\ \mathbf{Y}^W\end{bmatrix} \\ &= \begin{bmatrix}\boldsymbol{\mathcal{H}}^P & 0 \\ 0 & \boldsymbol{\mathcal{H}}^W\end{bmatrix}\begin{bmatrix}\mathbf{\Lambda}_{\sqrt{P^P}}\mathbf{X} \\ \mathbf{\Lambda}_{\sqrt{P^W}}\mathbf{X}\end{bmatrix} + \begin{bmatrix}\mathbf{V}^P \\ \mathbf{V}^W\end{bmatrix} \\ &= \begin{bmatrix}\mathbf{\Lambda}_{\sqrt{P^P}}\boldsymbol{\mathcal{H}}^P & 0 \\ 0 & \mathbf{\Lambda}_{\sqrt{P^W}}\boldsymbol{\mathcal{H}}^W\end{bmatrix}\mathbf{X}_1 + \begin{bmatrix}\mathbf{V}^P \\ \mathbf{V}^W\end{bmatrix} \\ &= \mathbf{A}\mathbf{X}_1 + \mathbf{B}\mathbf{V},\end{aligned} \tag{17}$$

where $\mathbf{X}_1 = \left[\mathbf{X}^T\mathbf{X}^T\right]^T$ and $\mathbf{V} = \left[\mathbf{V}^{P^T}\mathbf{V}^{W^T}\right]^T$. Also,

$$\mathbf{A} = \begin{bmatrix}\mathbf{\Lambda}_{\sqrt{P^P}}\boldsymbol{\mathcal{H}}^P & 0 \\ 0 & \mathbf{\Lambda}_{\sqrt{P^W}}\boldsymbol{\mathcal{H}}^W\end{bmatrix}$$

and

$$\mathbf{B} = \begin{bmatrix}\mathbf{I}_N & 0 \\ 0 & \mathbf{I}_N\end{bmatrix}.$$

A. Ergodic Channel Capacity: LTI PLC channel

The ergodic channel capacity of this fading channel composed of a LTI PLC channel and a LTV wireless channel is given by

$$\begin{aligned}C^{H,LTI} &= \max_{\mathbf{\Lambda}_{P^P},\mathbf{\Lambda}_{P^W}} \frac{B}{N}\mathbb{E}\{\log_2[\det(\mathbf{I}_{2N} + \mathbf{C}^H\mathbf{D}^{H^{-1}})]\} \\ &= \max_{\mathbf{\Lambda}_{P^P},\mathbf{\Lambda}_{P^W}} \int_0^\infty \cdots \int_0^\infty \log_2[\det(\mathbf{I}_{2N} + \mathbf{C}^H\mathbf{D}^{H^{-1}})] \times \\ &\quad p(|H^W[0]|^2, |H^W[1]|^2, \ldots, |H^W[N-1]|^2) \\ &\quad d|H^W[0]|^2, d|H^W[1]|^2, \ldots, d|H^W[N-1]|^2\end{aligned} \tag{18}$$

subject to $\mathrm{Tr}(\mathbf{\Lambda}_{P^P}) + Tr(\mathbf{\Lambda}_{P^W}) \leq P$, where

$$\begin{aligned}\mathbf{C}^H &= \mathbf{A}^H\mathbf{R}_{\mathbf{XX}}\mathbf{A}^{H^\dagger} \\ &= \begin{bmatrix}\mathbf{\Lambda}_{P^P}\mathbf{\Lambda}_{|\boldsymbol{\mathcal{H}}^P|^2} & 0 \\ 0 & \mathbf{\Lambda}_{P^W}\mathbf{\Lambda}_{|\boldsymbol{\mathcal{H}}^W|^2}\end{bmatrix}\end{aligned} \tag{19}$$

and

$$\begin{aligned}\mathbf{D}^H &= \mathbf{B}^H\mathbf{R}_{\mathbf{VV}}\mathbf{B}^{H^\dagger} \\ &= \begin{bmatrix}\mathbf{\Lambda}_{\sigma^2_{\mathbf{V}^P}} & 0 \\ 0 & \mathbf{\Lambda}_{\sigma^2_{\mathbf{V}^W}}\end{bmatrix}.\end{aligned} \tag{20}$$

B. Ergodic Channel Capacity: LTV PLC channel

The ergodic channel capacity of this fading channel composed of PLC and a wireless LTV channel is given by

$$\begin{aligned}C^{H,LTV} &= \max_{\mathbf{\Lambda}_{P^P},\mathbf{\Lambda}_{P^W}} \frac{B}{N}\mathbb{E}\{\log_2[\det(\mathbf{I}_{2N} + \mathbf{C}^H\mathbf{D}^{H^{-1}})]\} \\ &= \max_{\mathbf{\Lambda}_{P^P},\mathbf{\Lambda}_{P^W}} \int_0^\infty \cdots \int_0^\infty \int_0^\infty \cdots \int_0^\infty \log_2[\det(\mathbf{I}_{2N} + \mathbf{C}^H\mathbf{D}^{H^{-1}})] \times \\ &\quad p(|H^W[0]|^2, \ldots, |H^W[N-1]|^2)\ p(|H^P[0]|^2, \ldots, |H^P[N-1]|^2) \\ &\quad d|H^W[0]|^2, \ldots, d|H^W[N-1]|^2\ d|H^P[0]|^2, \ldots, d|H^P[N-1]|^2\end{aligned} \tag{21}$$

subject to $\mathrm{Tr}(\mathbf{\Lambda}_{P^P} + \mathbf{\Lambda}_{P^W}) \leq P$, where $\mathbf{C}^H$ and $\mathbf{D}^H$ are given by equations (19) and (20), respectively.

VI. NUMERICAL RESULTS

A. Channel models

A brief description of NB-PLC and NB-wireless channels is presented as follows:

NB-PLC channel model: Based on IEEE standard for low frequency narrow band PLC system [7], the frequency representation of a PLC channel is given by the following equation:

$$H(f) = \sum_{i=1}^{N_p} g_i e^{(-a_0 + a_1 f^k)d_i} e^{-j2\pi\frac{d_i}{v_0}}, \tag{22}$$

where N_p is the number of different paths that interferes between transmitter and receiver; g_i is a weighting factor that summarizes the reflection and transmission loss along a propagation path. It is a Gaussian random variable with zero mean and variance 1, which is scaled by 10000; $a_{0,1}$ are attenuation parameters that depend on the characteristics of the transmission line, such as impedance; k is the slope of attenuation with respect to frequency; d_i is a Gaussian random variable representing the length of propagation paths form transmitter to receiver (in meters) with mean d_a and standard deviation d_s. This value can not be smaller than d_m; and v_0 is the wave propagation speed in meters/second. For a NB-PLC channel, the adopted parameters are displayed in Table I [7].

TABLE I
NB-PLC SIMULATION PARAMETERS.

Parameter	Value
N_p	50
a_0	10^{-3}
a_1	2.5×10^{-9}
k	1
d_a	1000
d_s	400
d_m	100
v_0	$3 \times 10^{-8}/4$

NB-Wireless channel model: Due to the lack of models of a NB-Wireless in the frequency of 915 MHz, we obtained the NB-wireless channel, respectively, from a wideband wireless channel. This was done by filtering the wideband channel in the frequencies of interest. The model purposed follows 802.15.4a IEEE wireless channel model [8]. The channel impulse response (CIR) is given by

$$h(t) = \sum_{l=0}^{\infty} \sum_{k=0}^{\infty} \beta_{kl} e^{j\theta_{kl}} \delta(n - T_l - \tau_{kl}), \quad (23)$$

where β_{kl} is a Rayleigh distribution modeling the path gains, θ_{kl} is a uniform distribution from 0 to 2π modeling the randomness of path phases and, T_l and τ_{kl} are Poisson distributions modeling the cluster (with rate Γ) and ray (with rate γ) arrival time, respectively.

The channel model variables are given by

$$p(T_l|T_{l-1}) = \Lambda e^{[-\Lambda(T_l - T_{l-1})]}, \quad (24)$$

$$p(\tau_{kl}|\tau_{(k-1)l}) = \lambda e^{[-\lambda(\tau_{kl} - \tau_{(k-1)l})]}, \quad (25)$$

$$p(\beta_{kl}) = (2\beta_{kl}/\overline{\beta_{kl}^2}) e^{(-\beta_{kl}^2/\overline{\beta_{kl}^2})}, \quad (26)$$

$$\overline{\beta_{kl}^2} = \overline{\beta^2(0,0)} e^{-\frac{T_l}{\Gamma}} e^{-\frac{\tau_{kl}}{\gamma}}, \quad (27)$$

$$\overline{\beta^2(0,0)} = (\gamma\lambda)^{-1} G(1m) r^{-\alpha}, \quad (28)$$

$$G(1m) = G_t G_r \left[\frac{c}{4f\pi}\right]^2, \quad (29)$$

where c denotes the speed of light in meters/second.

The probability density function (pdf) of the small-scale amplitude, x, is

$$\text{pdf}(x) = \frac{2}{\Gamma(m)} \left(\frac{m}{\Omega}\right)^m x^{2m-1} e^{-\frac{mx^2}{\Omega}}, \quad (30)$$

where $m \geq 1/2$ is the Nakagami m-factor, $\Gamma(m)$ is the gamma function, and Ω is the mean-square value of the amplitude.

The parameter m is generated by independent Gaussian random variables with mean and variance given by, suggested in [8]

$$\mu(\tau_k) = 3.5 - \tau_k/73, \quad (31)$$

$$\sigma^2(\tau_k) = 1.84 - \tau_k/160, \quad (32)$$

in which τ_k is the ray delay measured in nanoseconds.

The used parameters are displayed in Table II. The parameters L and K denote the maximum number of clusters and rays, respectively. Note that, the parameters are given for a wide-band channel [8]. After the wideband channel is generated, it is filtered and its filtered frequency response is of our interest.

TABLE II
NB-WIRELESS SIMULATION PARAMETERS.

Parameter	Value
γ	20×10^{-9}
Γ	60×10^{-9}
λ	$1/(5 \times 10^{-9})$
Λ	$1/(300 \times 10^{-9})$
G_t, G_r	1
α	2.4
L	1
K	5

B. Numerical Results

For carrying out the simulations, we assume optimal power allocation (OA) over the subcarriers, this is done using the water-filling technique [10]. In Figs. 2 and 3, are plotted the PLC-wireless capacity versus $\beta = P^P/P$, for $P = 0$ and $P = 30$ dBm, respectively. Besides that, Fig. 4 shows the PLC, wireless and PLC-wireless capacities with the total transmission power $P = \{0, 10, 20, 30\}$ dBm.

The additive noise in PLC channel is modeled as a zero mean Gaussian random process ($v^P[n] \sim \mathcal{N}(\sigma_P^2, 0)$) while, the zero mean circularly symmetric complex Gaussian assumption is made for the wireless channel ($v^W[n] \sim \mathcal{N}(\sigma_W^2, 0)$). Also, $\|\mathbf{h}^W\|^2 = \|\mathbf{h}^P\|^2 = 1$ and $\sigma_W^2 = \sigma_P^2$ to guarantee a fair comparison, in which $\|.\|^2$ denotes 2-norm. All plots show the achievable data rate in terms of $\beta = P^P/P$ because $\beta = 0$ and $\beta = 1$ means that only wireless channel and PLC channel are used, respectively. Moreover, we assume $N = 2048$.

The following cases are numerically analyzed:

- H #1: We assume an LTI PLC channel and LTV wireless channel.
- H #2: We assume that both PLC and wireless channels are LTV.

Fig. 2 shows that the case H #1 has always a better achievable data rate than H #2. The value of β that maximizes the capacity is $\beta_{\max} \approx 0.7$, which means that 70% of the power should be allocated to the PLC signal, showing that the PLC channel performs better in this scenario. At Fig. 3, case H #1 has a better achievable data rate than H #2 for all values of β and $\beta_{\max} \approx 0.5$. Observing these figures, it can be noticed that for low values of P, case H #2 is better than H #1 in terms of achievable data rate. In opposite, for high values of P, case H #1 is better than H #2. As well, $\beta_{\max}$ tends to a half, i.e., the power allocation tends to be equally distributed between PLC and wireless signals as P increases.

Fig. 4 shows the achievable data rate of combinations mentioned before versus total transmission power in dBm. In this figure, PLC (LTI) means an LTI PLC channel, PLC (LTV) means an LTV PLC channel and WIR is the wireless channel, all of them using OA, see Table III. In addition, it exhibits the maximum PLC-wireless achievable data rate, i.e., for values of $\beta_{\max}$. At this figure, it can be noticed that H #1 and H #2 always have better achievable data rates than the sole use of PLC or wireless channel. Additionally, the achievable data rate enhances as the total transmission power increases.

TABLE III

LIST OF ABBREVIATIONS FOR PLOTS.

Description	Abbreviation
LTI PLC channel	PLC (LTI)
LTV PLC channel	PLC (LTV)
LTV wireless channel	WIR
LTI PLC and LTV wireless channel	H #1
LTV PLC and LTV wireless channel	H #2

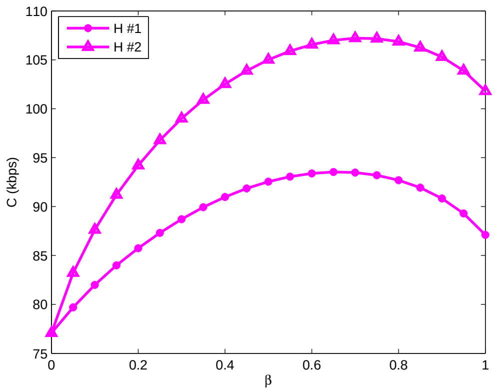

Fig. 2. Achievable data rate in cases H #1 and H #2 versus β for $P = 0$ dBm.

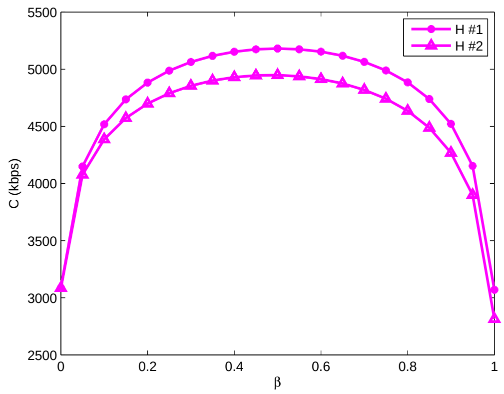

Fig. 3. Achievable data rate in cases H #1 and H #2 versus β for $P =$ 30 dBm.

VII. CONCLUSIONS

This work analyzed the performance gain adhered by the use of the existing diversity between ISM and NB-PLC frequency bands. Simulation results show that the achievable data rate gain when using a hybrid PLC-wireless, increases as the total transmission power increases.

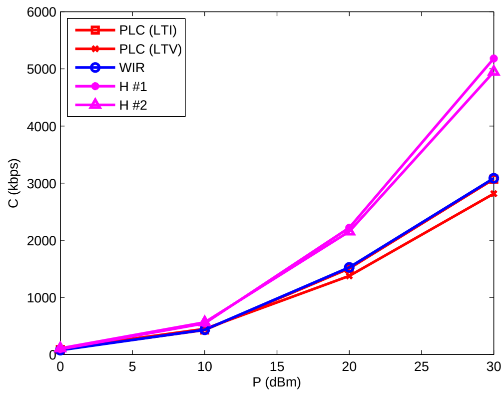

Fig. 4. Achievable data rate in cases H #1 and H #2 versus total transmission power.

Moreover, the attained results showed that for low values of total power transmission, case H #2 is better than H #1 in terms of achievable data rate. In opposite, for high values of total transmission power, case H #1 is better than H #2. As well, the allocated transmission power tends to be equally distributed between PLC and wireless signals as total transmission power increases. Also, it was observed that the sole use of PLC or wireless channel ($\beta_{\max} = 1$ or $\beta_{\max} = 0$) achieves a lower achievable data rate than the PLC-wireless scheme in all simulated scenarios.

ACKNOWLEDGMENTS

The authors would like to thank CNPq, CAPES, FAPEMIG, INERGE, Smarti9 Ltda. and Fulbright Commission for their financial support.

REFERENCES

[1] M. Kuhn, and A. Wittneben, "PLC enhanced wireless access networks: a link level capacity consideration," in *Proc. IEEE Vehicular Technology Conference*, 2002, pp. 125-129, vol. 1.
[2] M. Kuhn, S. Berger, I. Hammerström, and A. Wittneben, "Power line enhanced cooperative wireless communications," *IEEE Journal on Selected Areas in Communications*, vol. 24, no. 7, July 2006.
[3] S. Güzelgöz, H. B. Celebi, and H. Arsian, "Analysis of a multi-channel receiver: Wireless and PLC reception," in *Proc. Signal Processing Conference*, Aalborg, 2010, pp. 1106-1110.
[4] S. W. Lai, and G. G. Messier, "Using the wireless and PLC channels for diversity," *IEEE Transactions on Communications*, vol. 60, no. 12, pp. 3865-3875, Dec. 2012.
[5] S. W. Lai, N. Shabehpour, G. G. Messier, and L. Lampe, "Performance of wireless/power line media diversity in the office environment," in *Proc. IEEE Global Communications Conference*, Austin, TX, 2014, pp. 2972-2976.
[6] J. Lee, and Y. Kim, "Diversity relaying for parallel use of power-Line and wireless communication networks," *IEEE Transactions on Power Delivery*, vol. 29, no. 3, pp. 1301-1310, June 2014.
[7] *IEEE Standard for Low Frequency (less than 500 kHz) Narrow Band Power Line Communications for Smart Grid Application*, IEEE Std 1901.2^{TM}, 2013.
[8] A.F. Molisch et al., "IEEE 802.15.4a channel model - final report," IEEE 802.15 WPAN Low Rate Alternative PHY Task Group 4a, Tech. Rep., Nov. 2004.
[9] M. S. P. Facina, H. A. Latchman, H. V. Poor, and M. V. Ribeiro, "Cooperative in-home power line communication: analyses based on a measurement campaign," *IEEE Transactions on Communications*, vol. 64, no. 2, pp. 778-789, Feb. 2016.
[10] J. M. Cioffi, *Advanced Digital Communications Book*, Stanford University, 1987.